Materials Transactions, Vol. 57, No. 1 (2016) pp. 9 to 14

Influence of Minor Addition of Cr on the Magnetocaloric Effect in Fe-Based Metallic Ribbons

Daoqin Guo[1], Kang Cheung Chan[1,*] and Lei Xia[2]

[1]*Department of Industrial and Systems Engineering, Hong Kong Polytechnic University, Hung Hom, Hong Kong, China*
[2]*Laboratory for Microstructure, Shanghai University, Shanghai 200072, China*

$Fe_{84-x}Cr_xB_{10}Zr_5Gd_1$ ($x = 0, 2, 4, 6, 8$) ribbons were fabricated and their magnetocaloric effect was studied. The microstructure of the ribbons was found to change from crystalline to amorphous with the addition of Cr. The Curie temperature (T_C) undergoes an almost linear reduction (from 410 K to 300 K) and the peak magnetic entropy change, $|\Delta S_M^{peak}|$ (measured under a field of 1.5 T), first increases to a maximum value (from 0.70 J/kg K to 0.91 J/kg K) and then decreases to 0.66 J/kg K with increasing Cr content. The results further show that $Fe_{80}Cr_4B_{10}Zr_5Gd_1$ ribbon demonstrates good refrigerant capacity as large as 110 J/kg under a field of 1.5 T. With its T_C being close to room temperature and having a good refrigerant capacity, the Fe-based amorphous ribbon is a potential magnetocaloric material, although further work is needed to further improve the refrigerant capacity for industrial applications. [doi:10.2320/matertrans.M2015146]

(Received April 9, 2015; Accepted October 23, 2015; Published December 11, 2015)

Keywords: *amorphous materials, magnetic materials, X-ray diffraction, magnetic properties, microstructure*

1. Introduction

In 1860, William Thomson[1)] first discovered that the magnetization and temperature of a sample can affect each other in a reversible way. About twenty years later, Warburg[2)] firstly reported the magnetocaloric effect (MCE) of iron in which the temperature of iron increases when magnetized and the temperature decreases when iron is demagnetized. Despite the early discovery, research on the MCE had not been significant until Brown first realized in 1976 that magnetic refrigeration (MR) could be achieved around room temperature on the basis of the MCE.[3)] Fe-based metallic alloys have attracted wide attention due to their excellent soft magnetic properties since their first discovery in 1967 by Duwez.[4)] In recent decades, they have been receiving growing interest as potential working materials for room temperature magnetic refrigeration. Developing magnetic refrigeration in a room temperature range is an attractive way to reduce global warming, apart from improving the current gas compression/expansion cooling technology. MR is more energy-saving and environmentally-friendly when compared with conventional refrigeration.[5,6)] The coefficient of performance (COP), which is defined as the ratio of the heat removed from the cold reservoir to input work, of MR can reach 15, while vapor compression refrigeration only has COPs in the range 2∼6.[7)] Unlike the harmful gases in conventional refrigeration, the solid refrigerants and cooling water in MR do no harm to the environment. The MCE of working materials plays a critical role in the performance of MR. In order to compare the MCE of different materials, the refrigerant capacity (RC) has been acknowledged as a key function of two main parameters; the peak magnetic entropy change (ΔS_M^{peak}) and the working temperature range (ΔT).[8)]

Among various MCE materials, Fe-based amorphous materials, especially those with boron, have been widely investigated and proven to have potential to be applied for MR in the room temperature range.[9–19)] Compared with other promising candidates as magnetic refrigerants such as Gd-based amorphous materials which exhibit large ΔS_M^{peak} with narrow ΔT and a Curie temperature T_C much lower than room temperature,[20–23)] Fe-based amorphous materials display relatively small ΔS_M^{peak} but a much wider ΔT and an easily tunable T_C.[24,25)] In addition, iron is much cheaper and more abundant than gadolinium, which is an important issue for commercialization. Due to the poor glass forming ability (GFA) of Fe-based materials, current research in the field is mainly focused on metallic ribbons rather than bulk materials. It has also been shown that an effective way to improve their GFA and MCE is by adjusting the composition.[9–12,26)] In this study, research has been carried out to enhance the MCE of a Fe-based metallic glass by addition of Cr.

2. Experiment

Ingots of nominal composition $Fe_{84-x}Cr_xB_{10}Zr_5Gd_1$ ($x = 0, 2, 4, 6, 8$) were prepared in a copper mold casting machine. Ribbons, 0.05 mm thick and 1.5 mm wide, were fabricated by means of a melt spinning machine. The amorphous state of the as-quenched ribbons was characterized by X-ray diffraction (XRD) with Cu-Kα radiation. The magnetic hysteresis loops were measured to confirm the soft magnetic properties of the ribbon samples. The measurements were carried out using a Lakeshore 7407 vibrating sample magnetometer (VSM) under a magnetic field from −0.7 T to +0.7 T with 0.007 T per steps, both below and above the Curie temperature of the ribbon samples. The magnetocaloric effect of the amorphous ribbons was measured with VSM under a maximum applied magnetic field of 1.5 T with 0.005 T per steps at each constant temperature from 290 K to 430 K with 10 K per steps. The magnetic entropy change (ΔS_M) was calculated from one of the fundamental Maxwell's relations:[24)]

$$(\partial S(T, H)/\partial H)_T = (\partial M(T, H)/\partial T)_H, \quad (1)$$

where H is the magnetic field strength, T is the absolute temperature and M is the magnetization. Equation (1) can be integrated for an isothermal process:

*Corresponding author, E-mail: kc.chan@polyu.edu.hk

$$\Delta S(T, \Delta H) = \int_{H_1}^{H_2} (\partial M(T, H)/\partial T)_H \mathrm{d}H. \quad (2)$$

The entropy of a magnetic solid is contributed by the magnetic entropy, S_M, lattice entropy, S_{Lat}, and electronic entropy, S_{El}:

$$S(T, H) = S_M(T, H) + S_{Lat}(T) + S_{El}(T) \quad (3)$$

For an isothermal condition at a certain temperature T,

$$\Delta S_M(T, \Delta H) = \Delta S(T, \Delta H) = \int_{H_1}^{H_2} (\partial M(T, H)/\partial T)_H \mathrm{d}H \quad (4)$$

The refrigerant capacity (RC) was calculated by:

$$RC(\Delta H) = \int_{T_{cold}}^{T_{hot}} |\Delta S_M(T, \Delta H)| \mathrm{d}T. \quad (5)$$

Equation (5) can be easily approximately simplified to:

$$RC(\Delta H) = |\Delta S_M^{peak}| \times \delta T_{FWHM}. \quad (6)$$

where δT_{FWHM} is the full width at the half maximum of ΔS_M.

3. Results and Discussion

The XRD patterns of $Fe_{84-x}Cr_xB_{10}Zr_5Gd_1$ ($x = 0, 2, 4, 6, 8$) ribbons are shown in Fig. 1. As shown in the insert of Fig. 1, there are obvious sharp peaks in the XRD pattern of the $Fe_{84}B_{10}Zr_5Gd_1$ ($x = 0$) ribbon, suggesting that the structure of the sample is crystalline. For the XRD patterns of the $x = 2$, 4, 6 and 8 ribbons, a broad wave pack exists around $2\theta = 45°$ in each curve, which confirms the amorphous state of the ribbons. The microstructural difference between $x = 0$ sample and the rest ones is in good agreement with the basic empirical rules of Inoue for the formation of amorphous alloys:[27] with the addition of Cr in the system, the number of components increases. Consequently, the glass forming ability (GFA) of those metallic ribbons increases which makes the amorphous alloy formation easier. The magnetic properties of the ribbon samples with $x = 2, 4, 6, 8$ were characterized. For each ribbon sample, magnetization curves were measured from low temperature to high temperature for further calculation of their MCE. For illustration purposes, the typical magnetization curves of the $x = 2$ sample is shown in Fig. 2 ($1\,\mathrm{emu/g} = 1\,\mathrm{Am^2/kg}$). It shows that the saturation magnetization decreases with increase of temperature. In addition, the shape of the curves changes as temperature changes, which indicates the phase transition of all the ribbon samples are second order. Figure 3 shows the magnetic hysteresis loops of the ribbons at different temperatures. The magnetic hysteresis tests were carried out under a magnetic field ranging from $-0.7\,\mathrm{T}$ to $+0.7\,\mathrm{T}$, in $0.007\,\mathrm{T}$ steps. For each sample, the magnetic hysteresis loops were investigated at temperatures both before and after phase transition temperature, as can be seen in Fig. 2. All the hysteresis loops in Fig. 3 show small hysteresis and nearly zero coercivity, which indicates the excellent soft magnetic properties of the amorphous ribbons during their working temperature ranges. Additionally, the saturation magnetization around room temperature has a peak value when the Cr content are 4 mol in 1 mol Fe-based amorphous ribbons. On

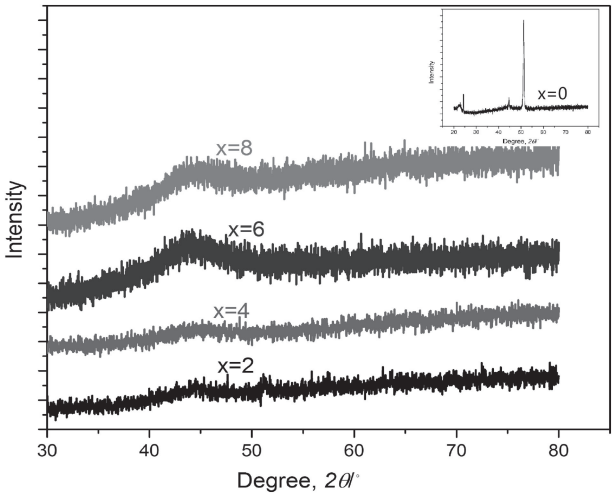

Fig. 1 The XRD results of $Fe_{84-x}Cr_xB_{10}Zr_5Gd_1$ ($x = 0, 2, 4, 6, 8$).

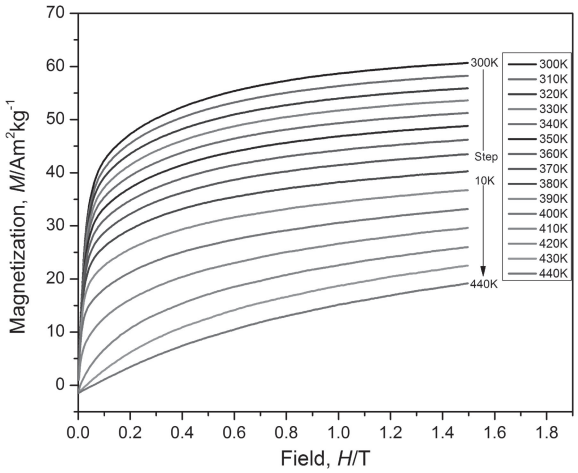

Fig. 2 Magnetization curves of sample $Fe_{82}Cr_2B_{10}Zr_5Gd_1$ from 300 K to 440 K.

the basis of the experimental magnetization curves and eq. (2), the $|\Delta S_M|$ vs. T curves were constructed as shown in Fig. 4. Each of the curves is shown to have a broad caret-like shape, illustrating the second order phase transition. The peak magnetic entropy change ($|\Delta S_M^{peak}|$) of each sample can also be readily obtained from the curves in Fig. 4. To compare the $|\Delta S_M^{peak}|$ of different metallic ribbons, a compositional dependence (which is actually the mole content of Cr) of the $|\Delta S_M^{peak}|$ curve was plotted as shown in Fig. 5. It reveals that the $|\Delta S_M^{peak}|$ value first increases and then decreases, when the Cr content increase from 2 mol to 8 mol. The peak value of $|\Delta S_M^{peak}|$ appears when the Cr content are 4 mol ($|\Delta S_M^{peak}| = 0.91\,\mathrm{J/kg\,K}$). The change of $|\Delta S_M^{peak}|$ is very similar to the result reported by Caballero-Flores.[19] In his work, the influence of Co and Ni addition on the $Fe_{88-2x}Co_xNi_xZr_7B_4Cu_1$ was studied. The simultaneous addition of Co and Ni makes $|\Delta S_M^{peak}|$ firstly increase and then decrease as x increases from 0 to 11, in steps of 2.75. Since the magnetic entropy change always peaks around the Curie temperature, the Curie temperature of each ribbon sample can be roughly obtained from Fig. 4. To obtain the Curie temperature more precisely, temperature dependence of

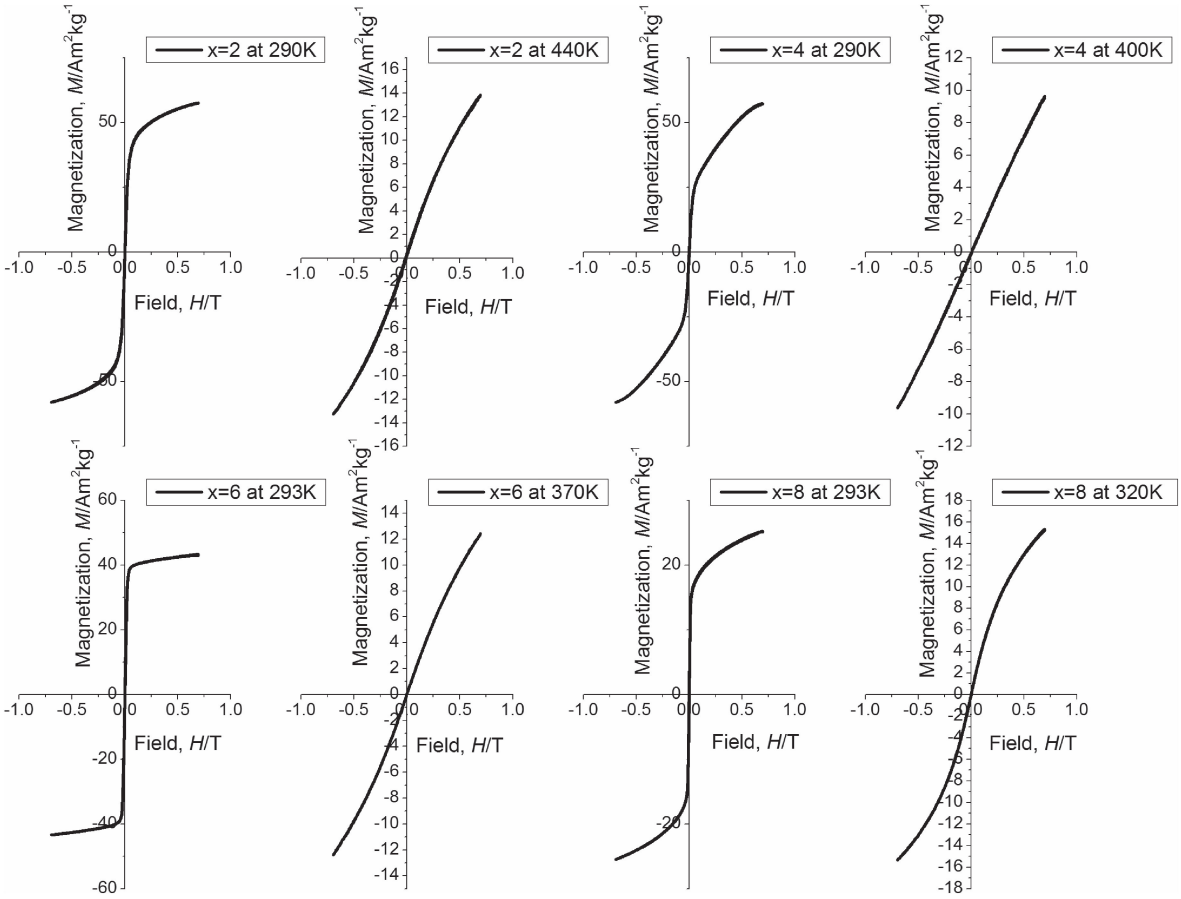

Fig. 3 Hysteresis loops of samples $Fe_{84-x}Cr_xB_{10}Zr_5Gd_1$ ($x = 2$, 4, 6 and 8) under different temperatures.

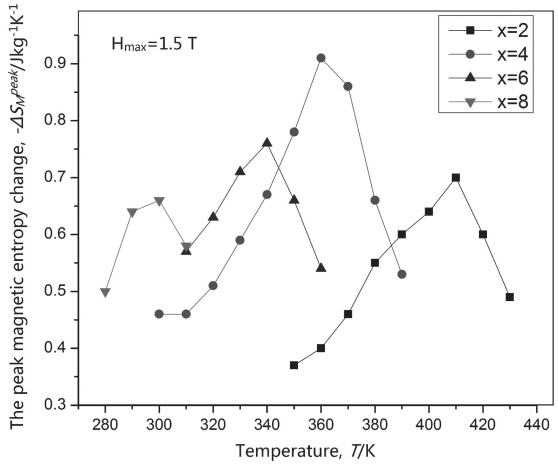

Fig. 4 The magnetic entropy change vs. temperature curves of the ribbon samples $Fe_{84-x}Cr_xB_{10}Zr_5Gd_1$ ($x = 2$, 4, 6 and 8).

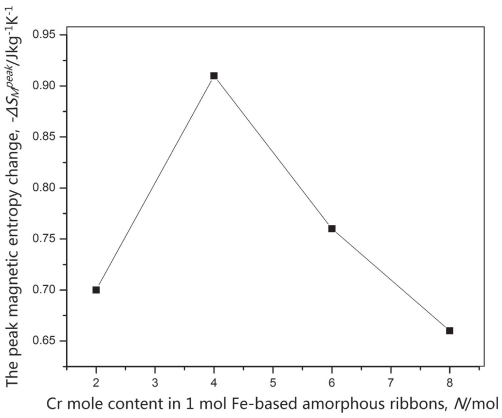

Fig. 5 The peak magnetic entropy change vs. the Cr mole content (from 2 mol to 8 mol) in 1 mol Fe-based amorphous ribbons curve.

magnetization curves were obtained during a cooling process and a typical curve for $Fe_{72}Cr_2B_{10}Zr_5Gd_1$ was plotted as shown in Fig. 6 for illustration purpose. Figure 6 was obtained under the cooling process from 440 K to 300 K at a field of 0.0323 T. The inset is temperature dependence of the derivative of the magnetization with respect to temperature (dM/dT) curve calculated from Fig. 6. The Curie temperature corresponds to the temperature where the value of dM/dT was minimum, which is 410 K. Figure 7 shows the experimental T_C vs. the mole content of Cr in 1 mol Fe-based amorphous ribbons curve indicated by the dark line with square dots. Differing from the change of $|\Delta S_M^{peak}|$, it can be noticed that T_C decreases nearly linearly when the Cr content increases from 2 mol to 8 mol (from 410 K to 300 K). The red dash line is the linear regression line with a slope of -17.5 K per Cr content ($T_C = [440 - 17.5 \times (Cr) \pm 10]$ K, where Cr represents for the Cr mole content in 1 mol Fe-based amorphous ribbons). This behavior can be explained by the negative exchange coupling between the Fe atoms with the newly introduced Cr atoms, which may be similar to the occurrence in some FeCr-based crystals.[28] The addition of Cr

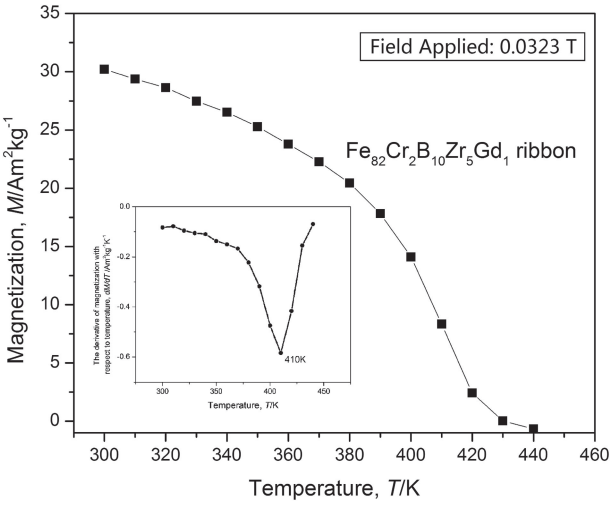

Fig. 6 Temperature dependence of magnetization curve of $Fe_{82}Cr_2B_{10}Zr_5Gd_1$ under the cooling process from 440 K to 300 K at a field of 0.0323 T.

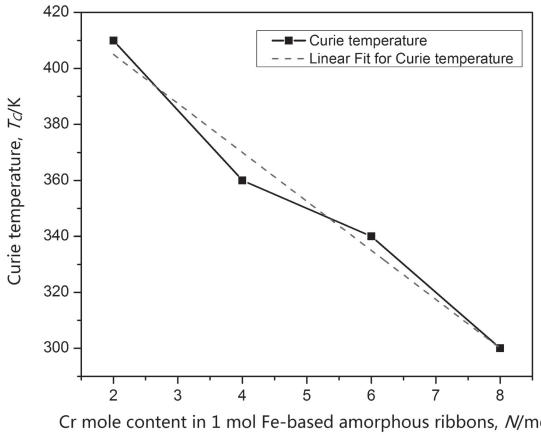

Fig. 7 The Curie temperature vs. the Cr mole content (from 2 mol to 8 mol) in 1 mol Fe-based amorphous ribbons curve.

Table 1 The magnetocaloric effect of the magnetic materials studied in this work and reported in the literature.

Nominal composition	Structure	Magnetic Field (T)	T_C (K) from the experimental results	T_C (K) from the linear results	δT_{FWHM} (K)	$\lvert\Delta S_M^{peak}\rvert$ ($J\,kg^{-1}K^{-1}$)	RC ($J\,kg^{-1}$)	Ref.
$Fe_{82}Cr_2B_{10}Zr_5Gd_1$	Amorphous	1.5	410	405	120	0.70	84	This work
$Fe_{80}Cr_4B_{10}Zr_5Gd_1$	Amorphous	1.5	360	370	120	0.91	110	This work
$Fe_{78}Cr_6B_{10}Zr_5Gd_1$	Amorphous	1.5	340	335	110	0.76	83	This work
$Fe_{76}Cr_8B_{10}Zr_5Gd_1$	Amorphous	1.5	300	300	110	0.66	73	This work
$Fe_{75}Nb_{10}B_{15}$	Amorphous	1.5	250	N/A	190	0.60	115	29)
$(Fe_{70}Ni_{30})_{89}Zr_7B_4$	Amorphous	1.5	342	N/A	N/A	0.70	N/A	17)
$Fe_{64}Mn_{14}CoSi_{10}B_{11}$	Amorphous	1.5	457	N/A	N/A	0.83	N/A	30)
$Fe_{72}Ni_{28}$	Amorphous	1.5	333	N/A	149	0.49	73	31)
$(Fe_{85}Co_{15})_{75}Nb_{10}B_{15}$	Amorphous	1.5	440	N/A	124	0.82	102	32)
$Gd_{55}Al_5Fe_{40}$	Amorphous	5.0	222	N/A	197	2.7	532	33)
$Gd_{60}Fe_{20}Co_{10}Al_{10}$	Amorphous	5.0	222	N/A	167	4.4	736	34)
$Gd_5Si_2Ge_2$	Crystalline	5.0	276	N/A	16.5	18.5	305	35)

atoms brings a decrease in the distance between Fe atoms, which results in antiferromagnetic interactions. Therefore, the Curie temperature decreases. With regard to the refrigerant capacity of each metallic ribbon, it can be obtained from eqs. (5) or (6). In this work, eq. (6) was used to calculate the RC in order to make it meaningful when compared with the results in the literature. The calculated RC results are listed in Table 1, together with the RC values of some other Fe-based as well as Gd-based metallic glasses reported in the literature. From the temperature dependence of the magnetic entropy change curves in Fig. 4, it is found that all of curves are relatively broad (large δT_{FWHM}), revealing that each ribbon has a wide working temperature range. This may compensate the effect of low peak magnetic entropy changes of Fe-based metallic glasses as compared to Gd-based materials when determining RC, which is shown in Table 1. From Table 1, it can be seen that both the $\lvert\Delta S_M^{peak}\rvert$ and RC of the $Fe_{84-x}Cr_xB_{10}Zr_5Gd_1$ ($x = 2, 4, 6, 8$) metallic ribbons are almost of the same order or even larger than the values of other reported Fe-based metallic alloys. Among the ribbons studied in this work, $Fe_{80}Cr_4B_{10}Zr_5Gd_1$ had the highest $\lvert\Delta S_M^{peak}\rvert$ (0.91 J/kg K) with δT_{FWHM} value of 120 K and RC value of 110 J/kg. Although both values of δT_{FWHM} and RC are same order as that of other reported Fe-based metallic alloys, the $\lvert\Delta S_M^{peak}\rvert$ is 51.6% larger than that of $Fe_{75}Nb_{10}B_{15}$, 30.0% larger than that of $(Fe_{70}Ni_{30})_{89}Zr_7B_4$, 9.6% larger than that of $Fe_{64}Mn_{14}CoSi_{10}B_{11}$, 85.7% larger than that of $Fe_{72}Ni_{28}$ and 11.0% larger than that of $(Fe_{85}Co_{15})_{75}Nb_{10}B_{15}$. On the basis of the comparison of δT_{FWHM}, RC values as well as $\lvert\Delta S_M^{peak}\rvert$, it could be concluded that $Fe_{82}Cr_4B_{10}Zr_5Gd_1$ is a promising MCE material.

Since the RC is influenced by the maximum magnetic field, comparison of the RC should be carried out under the same maximum applied magnetic fields. In order to better

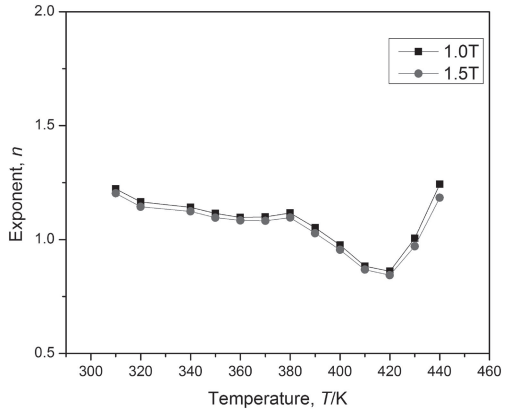

Fig. 8 Temperature dependence of the exponent for ribbon sample $Fe_{82}Cr_2B_{10}Zr_5Gd_1$ at two different maximum applied magnetic fields.

compare the MCE with other reported results measured under different maximum applied magnetic fields, the following expression,

$$|\Delta S_M(T, H)| = c(T)H^n, \quad (7)$$

is applied, where $c(T)$ is a constant.[19,36] According to this equation and the data from the magnetization curves, the exponent, n, for the $x = 4$ sample can be obtained from:

$$n = \mathrm{d}\ln|\Delta S_M|/\mathrm{d}\ln H. \quad (8)$$

Figure 8 shows the temperature dependence of the exponent, n, for the $x = 4$ sample under different applied fields, based on data collected under 0.5 T, 1 T and 1.5 T. The curves in Fig. 8 show that n is about 0.88 at T_C (360 K). Based on eq. (7) and this n value, the $|\Delta S_M^{peak}|$ value of $Fe_{80}Cr_4B_{10}Zr_5Gd_1$ becomes 2.63 J/kg K, when the maximum applied magnetic field increases to 5 T. It is larger than that of both $Fe_{77}Gd_3Cr_8B_{12}$ (2.31 J/kg K) and $Fe_{75}Gd_5Cr_8B_{12}$ (2.34 J/kg K) under 5 T.[37] Based on this $|\Delta S_M^{peak}|$ value, the RC of $Fe_{80}Cr_4B_{10}Zr_5Gd_1$ becomes 315 J/kg if δT_{FWHM} is assumed to be the same as that at 1.5 T. It is worth mentioning that δT_{FWHM} will also increase when the maximum applied magnetic field increases. The RC of $Fe_{80}Cr_4B_{10}Zr_5Gd_1$, therefore, will be much larger than 315 J/kg when H increases from 1.5 T to 5 T. This is very attractive as the well-known magnetic material, $Gd_5Si_2Ge_2$ only has a refrigerant capacity of 305 J/kg under 5 T as shown in Table 1.[35] Although it can be seen that the $|\Delta S_M^{peak}|$ of Fe-based magnetic materials is smaller than that of Gd-based magnetic materials in Table 1, the cost of Fe-based materials is much lower than that of Gd-based materials which is of great importance in mass production. Besides, the large δT_{FWHM} makes the RC of the Fe-based magnetic materials comparable to that of the Gd-based ones, and the Curie temperature of Fe-based materials are more suitable for room temperature applications. Moreover, the magnetocaloric effect of Fe-based materials can be optimized by adjusting the compositions on the basis of this work, which is being studied.

4. Conclusions

In this study, new Fe-based amorphous ribbons $Fe_{84-x}Cr_xB_{10}Zr_5Gd_1$ ($x = 2, 4, 6, 8$) were successfully fabricated and their magnetocaloric effect was investigated. The results show that the minor addition of Cr can affect both the peak magnetic entropy change and the Curie temperature of the Fe-based metallic ribbons. With increasing amount of Cr, the $|\Delta S_M^{peak}|$ can achieve a peak value and T_C decreases nearly linearly. The results show that the $Fe_{80}Cr_4B_{10}Zr_5Gd_1$ metallic glass achieves values of $|\Delta S_M^{peak}|$ 0.91 J/kg K and RC 110 J/kg at a T_C of 360 K. They are the highest $|\Delta S_M^{peak}|$ and the highest refrigeration capacity values near room temperature among all the Fe-based metallic glasses reported in the literature. Since both the peak magnetic entropy change and the Curie temperature are important factors for MCE materials, the $Fe_{80}Cr_4B_{10}Zr_5Gd_1$ metallic glass is shown to be a very promising MCE Fe-based material, and should be further investigated in regard to its MCE for commercial applications.

Acknowledgements

This research was fully funded by the Research Committee of the Hong Kong Polytechnic University under research student project account code RT4T.

REFERENCES

1) W. Thomson: Philos. Mag. **5** (1878) 4–27.
2) E. Warburg: Ann. Phys-berlin. **249** (1881) 141–164.
3) G. V. Brown: J. Appl. Phys. **47** (1976) 3673–3680.
4) P. Duwez: J. Appl. Phys. **38** (1967) 4096.
5) K. A. Gschneidner, Jr., V. K. Pecharsky and A. O. Tsokol: Rep. Prog. Phys. **68** (2005) 1479–1539.
6) K. Gschneidner, Jr. and V. Pecharsky: Annu. Rev. Mater. Sci. **30** (2000) 387–429.
7) K. A. Gschneidner and V. K. Pecharsky: J. Appl. Phys. **85** (1999) 5365.
8) M. E. Wood and W. H. Potter: Cryogenics **25** (1985) 667–683.
9) I. Škorvánek and J. Kováč: Czech. J. Phys. **54** (2004) Suppl. D, D189–D192.
10) F. Johnson and R. D. Shull: J. Appl. Phys. **99** (2006) 08K909.
11) V. Franco, A. Conde and L. F. Kiss: J. Appl. Phys. **104** (2008) 033903.
12) Y. K. Fang, C. C. Yeh, C. C. Hsieh, C. W. Chang, H. W. Chang, W. C. Chang, X. M. Li and W. Li: J. Appl. Phys. **105** (2009) 07A910.
13) A. Makino, T. Kubota, C. Chang, M. Makabe and A. Inoue: Mater. Trans. **48** (2007) 3024–3027.
14) Y. Wang and X. Bi: Appl. Phys. Lett. **95** (2009) 262501.
15) P. Álvarez, J. S. Marcos, P. Gorria, L. F. Barquín and J. A. Blanco: J. Alloy. Compd. **504** (2010) S150–S154.
16) J. Y. Law, V. Franco and R. V. Ramanujan: Appl. Phys. Lett. **98** (2011) 192503.
17) J. J. Ipus, H. Ucar and M. E. McHenry: IEEE Trans. Magn. **47** (2011) 2494–2497.
18) A. Waske, B. Schwarz, N. Mattern and J. Eckert: J. Magn. Magn. Mater. **329** (2013) 101–104.
19) R. Caballero-Flores, V. Franco, A. Conde, K. E. Knipling and M. A. Willard: Appl. Phys. Lett. **96** (2010) 182506.
20) Z. Zheng, X. Zhong, K. Su, H. Yu, Z. Liu and D. Zeng: SCIENCE CHINA Phys. Mech. Astronomy **54** (2011) 1267–1270.
21) L. Xia, K. C. Chan and M. B. Tang: J. Alloy. Compd. **509** (2011) 6640–6643.
22) S. Lu, M. B. Tang and L. Xia: Phys. B: Condens. Matter **406** (2011) 3398–3401.
23) H. Fu and M. Zou: J. Alloy. Compd. **509** (2011) 4613–4616.
24) V. K. Pecharsky and K. A. Gschneidner: J. Magn. Magn. Mater. **200** (1999) 44–56.
25) N. A. de Oliveira and P. J. von Ranke: Phys. Rep. **489** (2010) 89–159.
26) V. Franco, J. S. Blázquez and A. Conde: Appl. Phys. Lett. **89** (2006) 222512.

27) C. Suryanarayana and A. Inoue: *Bulk Metallic Glasses*, (CRC Press, Boca Raton, 2010).
28) D. Martínez-Blanco, P. Gorria, A. Fernández-Martínez, M. J. Pérez, G. J. Cuello and J. A. Blanco: J. Alloy. Compd. **509** (2011) S397–S399.
29) J. J. Ipus, J. S. Blázquez, V. Franco, A. Conde and L. F. Kiss: J. Appl. Phys. **105** (2009) 123922.
30) J. H. Lee, S. J. Lee, W. B. Han, H. H. An and C. S. Yoon: J. Alloy. Compd. **509** (2011) 7764–7767.
31) H. Ucar, J. J. Ipus, V. Franco, M. E. McHenry and D. E. Laughlin: JOM **64** (2012) 782–788.
32) J. J. Ipus, J. S. Blázquez, V. Franco and A. Conde: J. Alloy. Compd. **496** (2010) 7–12.
33) Q. Dong, B. Shen, J. Chen, J. Shen, F. Wang, H. Zhang and J. Sun: J. Appl. Phys. **105** (2009) 053908.
34) B. Schwarz, B. Podmilsak, N. Mattern and J. Eckert: J. Magn. Magn. Mater. **322** (2010) 2298–2303.
35) V. K. Pecharsky and J. K. A. Gschneidner: Phys. Rev. Lett. **78** (1997) 4494–4497.
36) V. Franco, A. Conde, J. M. Romero-Enrique and J. S. Blázquez: J. Phys. Condens. Matter **20** (2008) 285207.
37) J. Law, R. Ramanujan and V. Franco: J. Alloy. Compd. **508** (2010) 14–19.